Published in final edited form as:
ACS Chem Biol. 2015 January 16; 10(1): 146–156. doi:10.1021/cb500726b.

Changing the Selectivity of p300 by Acetyl-CoA Modulation of Histone Acetylation

Ryan A. Henry, **Yin-Ming Kuo**, **Vikram Bhattacharjee**, **Timothy J. Yen**, and **Andrew J. Andrews***

*Department of Cancer Biology, 333 Cottman Avenue, Fox Chase Cancer Center, Philadelphia, Pennsylvania, United States of America Andrew.andrews@fccc.edu. Phone: 215-728-5321

Abstract

Determining how histone acetylation is regulated is vital for treating the many diseases associated with its misregulation, including heart disease, neurological disorders, and cancer. We have previously reported that acetyl-CoA levels alter p300 histone acetylation in a site-specific manner *in vitro*. Here we further investigate how changing acetyl-CoA concentrations alter the histone acetylation pattern by altering p300 specificity. Interestingly, these changes are not a simple global change in acetylation, but rather site specific changes, whereby acetylation at some sites increase while others decrease. We also demonstrate how the p300 inhibitor C646 can pharmacologically alter p300 histone acetylation patterns *in vitro* and in cells. This study provides insight into the mechanisms regulating p300 residue specificity, a potential means for altering p300 dependent histone acetylation, and an investigation into altering histone acetylation patterns in cells.

INTRODUCTION

Understanding the regulation of histone acetylation has been a major goal in the fields of transcription and epigenetics. Misregulation of histone acetylation has been linked to neurological disorders, heart disease, and multiple forms of cancer [1-3], and thus understanding how the process of histone acetylation is regulated could play a key role in the treatment of these diseases. Complicating such investigations is the fact that many lysine acetyltransferases (KATs) can target several lysine residues within the histone [4-6]. As acetylation of different residues can result in different cellular events, it is important to understand the mechanisms that determine which histone residues a KAT will target. Unfortunately, technical constraints have previously limited the ability to observe acetylation of individual residues in a quantitative and efficient manner, hindering such an analysis. Utilizing a novel label-free mass spectrometry approach [5], we have overcome this technical limitation and are able to simultaneously determine the kinetics of histone acetylation at multiple residues of the histone.

Conflict of Interest The authors report no conflict of interest.

Supporting Information The steady-state experiments and kinetic parameters used to create many of the graphs found in the manuscript can be found in Supporting Information. This material is available free of charge via the Internet at http://pubs.acs.org.

Using this method, we previously demonstrated the differences in p300 and CREB-binding protein (CBP) specificity *in vitro* [6]. p300 and CBP are homologous lysine acetyltransferases, both of which are involved in numerous biological processes [7, 8], and each of which are responsible for the acetylation of several histone residues [7]. Specificity refers to the ability of a protein with multiple substrates to target one specific substrate (in the case of these KATs, their ability to target a particular lysine residue in the histone). The findings of our previous studies suggested that indeed p300 and CBP possess different propensities for acetylating specific residues on the histone (i.e. they possess different specificities). We also noted that p300 and CBP demonstrated varying degrees of cooperativity with acetyl-CoA, with different residues displaying different Hill coefficients. This observation implies that acetyl-CoA concentrations actually alter the residue preference of the enzyme. Thus, elucidating the extent to which this mechanism is capable of altering the specificity of p300 or CBP could provide a critical link between metabolic states, acetyl-CoA levels, and histone acetylation. Furthermore, tools or methodologies used to study the dependence of histone specificity on acetyl-CoA concentrations could further elucidate an important link between factors such as diet, metabolism, and gene regulation.

The importance of the relationship between acetyl-CoA levels and histone acetylation is underscored by the fact that cancer cells display abnormal metabolism and ATP synthesis (a phenomena referred to as the Warburg effect). This imbalance of ATP production can in turn lead to abnormal levels of acetyl-CoA in the cell[9]. Therefore, changes in metabolism could further alter proper histone acetylation states and could be a contributing factor in maintaining a cancerous state in the cell. Several recent studies have also demonstrated that acetyl-CoA levels fluctuate in an organism over time [10], and implicate the ability of acetyl-CoA levels to serve as a cellular regulatory mechanism [11-13]. Because of the role of acetyl-CoA levels in maintaining a healthy cell, it is important to understand how changes in acetyl-CoA levels can influence KAT activity and residue specificity.

In the case of p300 and CBP, we have observed different Hill values (or different degrees of cooperativity) for different residues. This means that the specificities of each site relative to one another (termed selectivity) will change along with the concentration of acetyl-CoA. In other words, while an enzyme may prefer to acetylate site A over site B at low acetyl-CoA concentrations, it could instead preferentially acetylate site B over site A at high acetyl-CoA concentrations. This is contrary to a classical model of cooperativity in which higher acetyl-CoA concentrations would result in a decrease in the rate of acetylation at less cooperative sites [14]. As this is not what we have observed, the most likely explanation is that the observed Hill coefficients are a result of monomeric cooperativity. The mechanism for monomeric cooperativity involves a slow transition between different enzyme conformations (referred to as E and E') [15]. In this case the enzyme can assume at least two different states: E, which can bind substrate (ES) and converts to E'S prior to product formation, and E' which, while less stable than E, is slow to transition back and allows for additional E'S to be formed, thus skipping the ES state [15-17]. Previous studies have indeed shown that the conformation of p300 changes in response to stimulatory factors [18], and therefore it is possible that such changes occur as a result of acetyl-CoA binding as well. Monomeric cooperativity was first described in metabolic enzymes such as hexokinase [16],

and many of the enzymes that have been found to display this behavior are also involved in metabolism. The acetyl-CoA-dependent cooperativity we have observed with p300 and CBP represents yet another example of monomeric cooperativity in a metabolic context.

The goal of this paper is to utilize a chemical biology approach to characterize this proposed monomeric cooperativity and to show that these effects can also be observed in cells. To do this, we used a small molecule inhibitor (C646) of p300 that competes with acetyl-CoA for binding to the enzyme [19]. We hypothesized that binding of C646 could stabilize the conformational change responsible for the observed cooperativity of p300. In other words, the binding of C646 to the acetyl-CoA binding pocket should impact the E to E' transition. C646 binds with higher affinity than acetyl-CoA[19]; if this facilitates the transition of E to E', we would predict an increase in enzyme activity under conditions where acetyl-CoA is able to displace C646 from E'. In support of this hypothesis, we show that low doses of C646 are able to stimulate p300, as long as acetyl-CoA is present in much greater concentrations than C646.

We note that in addition to activating p300, the presence of C646 also alters p300 selectivity. We refer to this alteration of selectivity and dependence on acetyl-CoA concentrations as "special selectivity." We utilize the information gained from *in vitro* assays to test whether the effects of special selectivity can be observed in cells. We accomplish this by utilizing C646 in cells under normal conditions, and under conditions where acetyl-CoA levels were lowered. The results of these experiments show that the special selectivity model does in fact hold true in cells, allowing us to increase the amount of acetylation at some sites while decreasing others.

This finding has wide reaching implications for the field of epigenetics and the study of histone modifications. We show that levels of acetyl-CoA not only affect the amount but also the pattern of histone acetylation. This provides an important link between metabolism, histone acetylation, and potentially cell signaling in response to metabolism. The consequence of special selectivity is that reducing the level of an enzyme's cofactors does not necessarily lead to a simple universal loss of activity but can actually result in higher levels of modification at specific sites, while still reducing the amount of modification at other sites. This suggests that KATs are not simply turned on and off, but rather their activities are altered by degrees through subtle changes. This property would provide cells with an exquisitely sensitive way to selectively change gene expression in response to small perturbations.

RESULTS AND DISCUSSION

p300 Acetylation has a Biphasic Dependence on C646

Our model suggests that p300 is undergoing conformational changes (from an E to E' state, where E' represents a more active conformation) that are stabilized by the binding of acetyl-CoA, or at least the occupation of the acetyl-CoA binding pocket. Distinguishing the stimulatory effect of a co-factor such as acetyl-CoA can be difficult, however, as it is a required component for acetylation. We therefore utilized the small molecule inhibitor C646, which binds to the acetyl-CoA binding pocket of p300 [19]. Based on the predictions of

our model, we hypothesized that when C646 concentrations are much less than acetyl-CoA, C646 could bind to p300 and facilitate the E to E' transition and thus increase the rate of acetylation at some sites once acetyl-CoA displaces C646 from the p300 E' state. To test this, we titrated C646 under saturating concentrations of $(H3/H4)_2$ tetramer and acetyl-CoA (or k_{cat} conditions) in order to determine how C646 affects the rate of acetylation of each site (Figure 1). We observed a biphasic dependence on the rate of C646 concentrations, where low concentrations of C646 had a stimulatory effect (Figure 1, Table 1, & Supplementary Figure 1), followed by an inhibitory effect at higher concentrations. We found that 1 uM of C646 caused a strong spike in acetylation of H3 at residues K14, K18 and K23 (Figure 1). 2.5 μM of C646 resulted in the maximal stimulation of H3K18 acetylation, while H3K14 peaked around 4 uM, and H3K23 around 2–3 uM of C646. The greatest degree of stimulation is on H3K23, where the rate increased ~7-fold over the DMSO control. Smaller degrees of stimulation were also observed on H4 at residues K5, K8, K12, and K16. The $K_{1/2}$s for activation ranged from ~90 nM to 1.5 μM and the $K_{1/2}$s for inhibition ranged from 1 to 5 μM, depending on the site being acetylated, with the highest activation occurring on residues in H3 (Figure 1 & Table 1).

For the purpose of comparison, we also determined the effect of C646 on CBP acetylation activity. We found that we only observed biphasic dependence for H3K18 (Supplementary Figure 2), whereas the other sites mainly displayed an inhibitory effect. Additionally, we found that this stimulation of CBP occurred over a much smaller range of C646, and was inhibited at much lower concentrations of C646 than p300 (within the nanomolar range). For this reason, the remainder of our investigation focused on the effects seen with p300.

C646 Alters Acetylation in Cells

We next sought to validate the *in vitro* data by testing the effects of C646 on acetylation patterns in cells. We therefore performed a titration of C646 in BxPC3 (human pancreatic cancer) cells (Figure 2 & Supplementary Figure 3). At 4 hours after treatment, consistent with our *in vitro* work, histone acetylation increased at several residues, most notably on histone H3. Also in agreement with our *in vitro* data, the greatest increase in acetylation was observed on H3K18 and H3K23 (Figure 2). On H3K18 we saw a ~2.5-fold increase in acetylation (Figure 2B), while on H3K23 we saw a ~1.5-fold increase (Figure 2C). Interestingly, the ratio in the fold increase between K18 and K23 acetylation was close to that of the ratio of the k_{cat} values (~1.6-fold), suggesting that the free acetyl-CoA concentration in cells is much higher than the ~15 μM $K_{1/2}$ values observed by steady-state kinetics. It is also interesting to note that the maximum stimulation by C646 on H4K5 and H4K8 *in vitro* and in cells were very similar. From these experiments we also determined an apparent EC_{50} for activation and an apparent IC_{50} of inhibition. H3K18 and H3K23 have similar apparent EC_{50} values, of approximately 0.4 μM (Supplementary Table 1), while H3K18 has a larger apparent IC_{50} of ~6.8 μM compared to H3K23 with an apparent IC_{50} of ~3.3 μM, suggesting that acetylation of H3K18 persists over a larger range of C646 concentrations than H3K23.

As a basis of comparison for the effects of C646, we also performed several experiments with the histone deacetylase inhibitor TSA. Histone deacetylase inhibitors (HDACi) are

currently popular potential anti-cancer therapeutics [20, 21]. While HDAC inhibitors increase acetylation at the majority of acetylation sites, the ability to increase acetylation at specific sites would better enable us to determine the role of those sites *in vivo*, and possibly lead to new treatment ideas, with fewer adverse effects. For this reason, we were interested in understanding how C646 treatment compared to an HDAC inhibitor in terms of changes to the histone acetylation pattern.

Consistent with previous reports, TSA globally increased acetylation at each site of H3 (Table 2). What is interesting is that C646 works in a much more site-specific manner than TSA: For example, C646 is about 50% as effective as TSA at stimulating acetylation of H3K18. Meanwhile, TSA has a much greater effect on H3K9 acetylation, increasing acetylation of this site 42-fold more than C646. In this way, treatment with a drug such a C646 provides a more targeted approach to altering histone acetylation than an HDAC inhibitor such as TSA. This seems intuitive because C646 targets one of multiple KATs, while HDACi act on deacetylases and thus the effect seen with an HDACi is the sum of many KATs, as opposed to C646, which selectively targets p300. Therefore, these site-specific changes that result from C646 treatment have the potential to be more amenable to be utilized for therapeutic purposes than the global changes that are seen with HDAC inhibitors. This would be ideal for treatment of diseases that are associated with, for example, deficiencies in H3K18 acetylation [22].

Finally, to confirm that the observed changes in acetylation in cells in response to C646 are caused by p300, we performed a titration of C646 in BxPC3 cells depleted of p300 via stable integration of a p300 shRNA (Figure 3A). Due to their slow growth, we chose several key concentrations of C646 from our previous titration. Compared to parental cells, there was a general decrease in histone acetylation in the p300 knockdown cells, with H3K9 and H3K14 acetylation dropping to about 50% of the wild-type level. Interestingly, there was an increase in H3K18 acetylation in the p300-depleted cells. We have previously shown that CBP preferentially targets this site [6], so this increase could be due to a compensatory activity of CBP in the absence of p300.

In the p300-depleted cells, the effects of C646 were dramatically different from the parental cells. At relatively low doses of C646, we observed a significant decrease in acetylation at H3K14, H3K18, and H3K23 (Figure 3 B-D). Acetylation at these sites was reduced by 80% of that seen in the control, as compared to the parental BxPC3 cells, where we saw up to a 2.5 fold stimulation of acetylation. Although there are slight variations in acetylation levels, in each of the C646 treated p300-depleted cells, we see an inhibitory effect from C646. These results indicate that p300 is responsible for the increase in acetylation in parental BXPC3 cells treated with C646. The inhibition we observed in the p300 knockdown cells, therefore, is likely due to the inhibitory effect of C646 on CBP.

Cell Starvation Ablates the Stimulatory Effect of C646 in Cells

In our model, C646 is able to stimulate p300 histone acetylation because it induces conformational changes in the enzyme. We therefore predicted that if we depleted acetyl-CoA levels in the cell, C646 would be less effective in stimulating activity. This is due to the fact that the on-rate for acetyl-CoA is dependent on the concentration of acetyl-CoA and

therefore at lower concentrations there is more time for both the enzyme to convert back to its original pre-C646 state, and for C646 to rebind. The prediction, therefore, was that reduced acetyl-CoA would lead to C646 inhibiting acetylation. Two methods were used to reduce acetyl-CoA levels in the cell: cells were either serum starved for 16 hours or treated with MEDICA 16 (an inhibitor of ATP-citrate lyase, an enzyme responsible for producing acetyl-CoA from citrate) prior to treatment with C646 [23-25]. After starvation, BxPC3 cells were treated with either C646 (Figure 4) or TSA (Table 2). We utilized TSA here as a positive control, as even under conditions of limited acetyl-CoA, TSA should still cause increased histone acetylation when compared to untreated cells. After serum starvation, C646 concentrations that normally stimulated acetylation were indeed found to inhibit acetylation at K9, K14, K18, and K23 in H3 (Figure 3). As predicited, TSA treatment increased levels of histone acetylation in the serum starved cells (Table 2). Treatment with MEDICA 16 did not result in inhibition of acetylation, but instead resulted in a muted stimulatory response to C646. As ATP-citrate lyase is only one potential source of acetyl-CoA in the cell, MEDICA 16 may not reduce acetyl-CoA levels as efficiently as serum starvation. Therefore, instead of causing C646 inhibition of acetylation, MEDICA 16 only reduced the degree of stimulation caused by C646.

Modeling the Effects of Acetyl-CoA on p300 Specificity and Selectivity

After confirming that acetyl-CoA levels influence histone acetylation patterns, with both purified p300 and in cells, we sought to develop a more accurate model for the influence of acetyl-CoA concentration on p300 specificity. To accomplish this, we performed steady-state experiments with p300 at several different concentrations of C646. For these experiments, we selected concentrations on either side of the peak of activation that we observed for residues on H3. We first performed a DMSO control, for a baseline (Figure 5) and then selected C646 concentrations of 0.5, 2.5 and 5 μM (Figure 6, and Supplementary Figures 4 & 5). From these steady-state experiments, we obtained the kinetic parameters from which specificity is derived. Specificity is the ability of an enzyme to target a specific substrate, or in the case of p300, to target a specific lysine residue. This parameter is usually reported as k_{cat}/K_m^{nH} [26]. Selectivity is the ability of p300 to target one specific residue relative to another residue. While k_{cat}/K_m^{nH} is an accurate definition of specificity [5, 26], the value of k_{cat}/K_m^{nH} changes depending on $[S]^{nH}$, or the concentration of the substrate raised to the power of the Hill coefficient. While typically choosing units relative to concentrations that might exist *in vivo* solves this [26], this is not entirely accurate for p300. The problem here is that between 0 and 100 μM acetyl-CoA, the selectivity of p300 changes. Additionally, these changes in selectivity are within the reported physiological range of acetyl-CoA: 5–50 μM [27, 28]. An alternative and more accurate picture of specificity, then, is to view the free energy of catalytic proficiency ($\Delta\Delta G_{cp}$) [5], or the ratio of catalytic efficiency (k_{cat}/K_m^{nH}) to the rate of nonenzymatic acetylation (k_{nE}) as a function of acetyl-CoA concentration ($\Delta\Delta G_{cp} = -RT\ln([\text{Acetyl-CoA}]^{nH-1}((k_{cat}/K_m^{nH}) / k_{nE}))$ (Figure 7 and Supplementary Figure 6), and to do so at each individual site. In this equation, noncooperative (nH=1) acetylation results in a $\Delta\Delta G°$ which is independent of concentration (horizontal line) and apparent cooperativity results in a $\Delta\Delta G°$ which will change as a function of acetyl-CoA. Using this method, we can also visualize changes in selectivity, which occur when one line intersects another. This model provides a clear way of viewing

both specificity for a particular residue as a function of acetyl-CoA and shows how the selectivity can change between residues.

Using this methodology, we first examined the selectivity of p300 in our DMSO control (Figure 7 A &B). We observed that those sites that demonstrated cooperativity had a more favorable (more negative) free energy as acetyl-CoA concentrations increased. As suggested above, the fact that all sites did not have identical dependences on acetyl-CoA concentrations (different Hill coefficients), leads to changes in the energetic favorability. For example, when looking at the DMSO control (Figure 7 A & B) H3K9, had the least favorable free energy at low acetyl-CoA levels while having the most at saturating acetyl-CoA. In contrast, the addition of C646 suppressed H3K9 acetylation in favor of acetylation of H3K18, H3K23 and H4K5 (Figure 7 C & D). The graphs created for this type of analysis provide a more complete picture into the selectivity of an enzyme like p300, and provide a visual map for understanding special selectivity, showing the points where acetyl-CoA concentrations are altering the specificity and the selectivity between residues.

It is worth noting that these graphs represent situations where acetyl-CoA levels are limiting, until reaching the highest levels of acetyl-CoA. At these high concentrations, selectivity correlates with k_{cat}. As noted above, we observe that the change in acetylation rate between K18 and K23 in the presence of C646 is similar in cells to the change observed under k_{cat} conditions. This suggests that local concentrations of acetyl-CoA in the cell are high, an interesting observation that comes from observing special selectivity in this way.

To summarize these results, we have shown that C646, previously reported as an inhibitor of p300, actually has a biphasic effect on p300 acetylation, stimulating activity at low concentrations of C646 relative to acetyl-CoA, while inhibiting at higher concentrations. We have shown that similar changes in histone acetylation can be observed in cells and that the cellular response to C646 is acetyl-CoA dependent. We have also demonstrated the importance of observing KAT selectivity as a function acetyl-CoA. Understanding how specificity and selectivity of a KAT such as p300 can be regulated and, importantly, experimentally altered, provides valuable information for treating diseases that arise as a result of aberrant histone acetylation. In the same way, understanding how acetyl-CoA concentrations regulate KAT function is important to understanding how cellular metabolism and changes to acetyl-CoA concentration can affect the epigenetic state of a cell.

Of great interest is the ability of C646 to alter p300 specificity and selectivity. The simplest mechanism for this C646-dependent change is that p300 exists in multiple conformations that dictate specificity and selectivity. The presence of C646 alters the equilibrium between these different conformations such that binding of C646 at low concentrations may help to stabilize certain conformations that, in the presence of acetyl-CoA, will promote acetylation of certain sites. Similarly, one conformation of p300 could have a lower affinity for C646, and after the transition occurs, is less likely to be bound by C646, allowing the enzyme to escape inhibition. This model accounts for the stimulation that we see at low C646 concentrations, while still providing an explanation for the inhibition that occurs at higher concentrations. Further strengthening our model is the observation that cell starvation and

treatment with MEDICA 16 ablates or decreases, the stimulatory effect observed with C646. If acetyl-CoA is in fact able to outcompete C646 at lower concentrations of C646, then it stands to reason that lowering acetyl-CoA levels would result in C646 remaining bound to p300, which leads to the decrease in histone acetylation that we observed in serum starved cells. Our concern that the cellular effects of C646 may be complex to interpret was ameliorated by the fact that knockdown of p300 from BxPC3 cells lead to a loss of the C646 stimulatory effect. Thus, we conclude that C646 stimulatory effects in cells are, in fact, due largely to its actions on p300.

We have also compared the effect of C646 to the HDAC inhibitor TSA and found that TSA has a large effect on the majority of sites, while C646 has little effect on H3K9 (42-fold < TSA), while still being 50% as effective at H3K18 as TSA. This experiment reveals an important advantage to targeting KATs for therapeutic purposes instead of HDACs. While HDAC inhibitors clearly cause a larger increase in histone acetylation, this increase is at the majority of sites, and thus lacks the selectivity that maybe critical for achieving therapeutic outcomes. Studies have shown difficulties working with HDACi because of their numerous side effects, from cardiovascular problems like heart arrhythmias, reduced fertility, and even several neurological problems [29, 30]. This may be due to the fact that if HDACs are underactive, there is no redundancy to compensate for their inactivity: acetyl groups will remain on the histone and will continue to accumulate with no means for their removal. Meanwhile, if a KAT is too active, there are HDACs in the cell to compensate and remove these marks. Therefore, KATs may be a more viable target for therapeutic intervention than HDACs, as they appear to produce less global perturbations to histone acetylation patterns.

The data presented here underscores the importance of acetyl-CoA concentration in determining KAT specificity. The concept of special selectivity presents interesting possibilities for regulating acetylation *in vivo*. In essence, changing the amount of acetyl-CoA available in a reaction, or more importantly in a cell, will lead to changes in the extent of acetylation at each site. Utilizing a mass spectrometry-based technique that looks at each site of acetylation simultaneously has allowed us to determine the kinetics of p300. This in turn allowed us to create a special selectivity map, demonstrating that we can alter the dependence of p300 on acetyl-CoA levels by using different concentrations of C646. This means at a set concentration of acetyl-CoA, we could alter the p300 acetylation preference, or alternatively, that C646 could be utilized to alter the point at which specificity changes over a range of acetyl-CoA concentrations. By further characterizing the selectivity changes of different KATs, we could better understand how to regulate their activity through means such as limiting acetyl-CoA concentrations. It is also possible that such a mechanism exists *in vivo*: it has recently been demonstrated that during early development, a cell undergoes changes to acetyl-CoA levels, which also correlate with changes to histone acetylation [10]. Based on our findings, it possible that these changes in acetyl-CoA could affect p300 selectivity, and correlate with changes in the histone acetylation pattern. This would be a useful mechanism for regulating gene expression during early development.

The identification of C646 as a modulator of p300 activity in itself is interesting as it is contrary to the common-held perception of it as an inhibitor. The fact that an enzyme can escape an inhibitor via altered specificity presents both problems and opportunities for

therapeutic intervention. Inhibitor escape is dependent on conformational flexibility, which is in turn linked to the concept of special selectivity. Understanding how this process occurs, therefore, has the potential to allow for pharmacologically retargeting an enzyme to different lysine residues or substrates. These results also challenge the commonly held practice of finding the highest tolerable dose of a drug. This suggest that drugs affecting special selectivity might be more effective at certain concentrations, with higher concentrations producing different or even unwanted effects.

The data presented here advances our understanding of how KAT specificity can be regulated. We have shown that C646 can actually stimulate acetylation at low doses, altering both the specificity and selectivity. We have also demonstrated the fluid nature of p300 specificity, how it relies on acetyl-CoA concentrations, and how this acetyl-CoA dependence can be altered through the use of C646. We have demonstrated that this acetyl-CoA dependence exists in cells, and have shown how changes in acetyl-CoA not only alter histone acetylation, but also can be used to change how a cell responds to drug treatment. The elucidation of special selectivity, the ability of an enzyme's selectivity to change, coupled with the discovery of a modulator of p300 activity raises important questions of how drug dose influences the efficacy of potential KAT inhibitors, and how these effects could be utilized to manipulate aberrant histone modification patterns to treat the diseases associated with this aberrant acetylation.

METHODS

Reagents

All Chemicals were purchased from either Sigma-Aldrich or Fisher Scientific; the purity was the highest commercial grade available or met LC/MS grade. Ultrapure water was generated from a Millipore Direct-Q 5 ultrapure water system. Recombinant histone H3 and H4 were purified and provided from the Protein Purification Core at Colorado State University. Acetyl-CoA was obtained from Sigma-Aldrich. C646 was purchase from EMD Millipore.

Protein purification

p300 and CBP were expressed and purified from Sf9 cells as previously described [6]. The p300 construct was graciously provided by Karolin Luger (Colorado State University).

C646 titrations (k_{cat} conditions)

Titrations of C646 were performed in buffer containing 100 mM Ammonium bicarbonate and 50 mM HEPES buffer (pH 7.8) at 37°C. All reactions were performed in the presence of 0.2% DMSO. Experiments were done under k_{cat} conditions, utilizing excess H3/H4 (15 μM) and acetyl-CoA (200 μM) in the presence of p300 (5 – 10 nM) or CBP (5 nM). C646 concentrations were varied between 0.1 – 5 μM. Assays were quenched using four volumes of trichloroacetic acid (TCA). The precipitate was then washed twice with 150 μL acetone (−20°C) [31]. Samples were dried, 2 μL propionic anhydride was added, and ammonium hydroxide was used to quickly adjust the pH to ~ 8 [32]. Samples were then incubated at 51°C for 1 h followed by trypsin digestion (overnight at 37°C).

Enzymatic kinetics assays for p300 and CBP

Steady-state kinetics for the H3/H4 tetramer were performed as described above. However, steady-state assays contained varying amounts of p300 ranging from 2 to 10 nM, 5 nM CBP, 15 μM H3/H4 and varying levels of acetyl-CoA (1 – 200 μM). All kinetics assays were performed in the presence of 0.2% DMSO, with either no drug, 0.5, 2.5, or 5.0 μM of C646.

Treatment of BxPC3 pancreatic cancer cells with C646 and TSA

BxPC3 cells were treated with either a 0.2% DMSO control, varying concentrations of C646 (0.1 – 50 μM) in 0.2% DMSO, or 0.5 μM TSA in 0.2% DMSO. Cells were treated for 4 hours before harvesting. Histones were extracted overnight from the cell pellet using 0.2 N HCl. Extracted histone was then prepared with propionic anhydride and treated with trypsin as described above. Cell starvation involved switching the cells to a serum-free media for 16 hours prior to treatment, and returning to media containing serum during drug treatment. Treatment with 5 μM MEDICA 16 was done for 24 hours prior to C646 treatment. TSA and MEDICA 16 were obtained from Sigma-Aldrich.

Production of BxPC3 p300 knockdown cells

BxPC3 p300-depleted cell lines were created via lentiviral infection of a p300 shRNA (Dharmacon TRCN0000039883). Lentivirus was produced using HEK293T host cells co-transfected with the p300 TRCN0000039883 shRNA plasmid, lentiviral packaging plasmid pCMV-cR7.74psPAX2, and envelope plasmid pMD2.G. BxPC3 cells were infected with the virus and subjected to puromycin (2.5 μM) selection for 7 days. The surviving cells were then pooled and tested for p300 knockdown by Western blotting using a p300 antibody (Santa Cruz Biotechnologies, SC-584) with alpha-tubulin as a loading control (Sigma, mouse monoclonal T5168).

UPLC-MS/MS analysis

A Waters Acquity H-class UPLC (Milford, MA) coupled to a Thermo TSQ Quantum Access (Waltham, MA) triple quadrupole (QqQ) mass spectrometer was used to quantify acetylated H3/H4 peptides as previously described [5, 6].

QqQ MS data analysis

Each acetylated and/or propionylated peak was identified by retention time and specific transitions, as previously reported [5, 6]. The resulting peak integration was done using Xcalibur software (version 2.1, Thermo). The fraction of a specific peptide (F_p) is calculated by eq. 1, where I_s is the intensity of a specific peptide state and I_p is the intensity of any state of that peptide, and analyzed as previously described [5, 33].

$$F_P = I_S / \left(\sum I_P \right) \quad \text{(Eq.1)}$$

Data analysis

All models were fit to the data-using Prism (version 5.0d). The initial rates (v) of acetylation were calculated from the linear increase in acetylation as a function of time prior to 10% of

the sum of acetylated residues. To measure steady-state parameters for acetyl-CoA, the initial rates were calculated based on time points where less than 10% of the acetyl-CoA was consumed (based on a coupled assay [34]) and where the acetylated H3/H4 fraction is less than 0.1 times the fraction of unacetylated H3/H4. k_{cat}, $K_{1/2}$, and the Hill coefficient (nH) were determined by fitting the equation:

$$\frac{v}{[E]} = k_{\mathrm{cat}(app.)} \frac{[S]^{nH}}{\left([S]^{nH} + K^{nH}_{(\mathrm{app})}\right)} \quad \text{(Eq.2)}$$

where [S] is the concentration of substrate (here, acetyl-CoA), and [E] is the concentration of enzyme (either CBP or p300). The nH was assumed to be one unless the data dictated otherwise, in which case the nH was confirmed by the equation:

$$Log\,[\mathrm{f}/(1-\mathrm{f})] = nH^{*} Log\,[\mathrm{S}] + \mathrm{C} \quad \text{(Eq.3)}$$

where f is the normalized change in v/[E]. When determining the nH for the 4 different concentrations of C646, wherever possible, the data was fit simultaneously to create a shared Hill Coefficient for all fits at any given site. This method was not utilized for H3K9 or H4K5, where only one treatment displayed cooperativity while the rest did not, and was also not utilized for H4K16, where the Hill coefficients varied too greatly among treatments to utilize a single fit.

Selectivity of multiple sites

In order to understand selectivity, it is important to remember in these experiments all substrates are present at once. This means the denominator for the v/E equation for any one site is the same. Therefore, specificity is reduced to k_{cat}/K_{mnh} times the concentrations of S raised to the Hill (for details, see [5]). However, given that we have 8 possible sites of acetylation, it is easier to utilize free energy change of catalytic proficiency, Eq. 4, where k_{nE} is the nonenzymatic rate of acetylation.

$$\Delta\Delta G_{cp} = -\boldsymbol{RT} ln \left([S]^{nH-1} \frac{k_{\mathrm{cat}}/K_m^{nH}}{k_{nE}} \right) \quad \text{(Eq.4)}$$

In Eq. 4 the second order rate for nonenzymatic acetylation (k_{nE}) is not cooperative, so dependence on S is based on the Hill coefficient for catalytic efficiency minus one. This reduces the selectivity to the difference in free energy for any two sites.

Biphasic fit

To determine the $K_{1/2\ (activation)}$ and the $K_{1/2\ (inhibition)}$, data was fit using the following equation, assuming an equilibrium between enzyme (E) and inhibitor (I) that is activating, and a second concentration that is inhibiting:

$$\frac{v}{[E]} = \frac{k_{\mathrm{initial}}{}^{*} K_a{}^{*} K_i + k_{\mathrm{act}}{}^{*} [I]^{*} K_i}{K_a{}^{*} K_i + [I]^{*} K_i + [I]^{*} K_a} \quad \text{(Eq.5)}$$

Supplementary Material

Refer to Web version on PubMed Central for supplementary material.

Acknowledgements

We thank Dr. P. Cole and Dr. K. Wellen for their input and feedback in the preparation of this manuscript. This work was supported by a grant from the Pennsylvania Department of Health. The Pennsylvania Department of Health specifically disclaims responsibility for any analysis, interpretations, or conclusions. R.A.H. was supported by NIH Training Grant 2T32 CA-009037. T.J.Y. was partly supported by NIH CA169706, CA182651, Core grant CA06927, PA Cure, generous donations by Mrs. C. Greenberg, and the Bucks County Board of Associates. V.B. was supported by a Pancreatic Cancer Action Network/AACR postdoctoral fellowship.

References

1. Gayther SA, Batley SJ, Linger L, Bannister A, Thorpe K, Chin SF, Daigo Y, Russell P, Wilson A, Sowter HM, Delhanty JD, Ponder BA, Kouzarides T, Caldas C. Mutations truncating the EP300 acetylase in human cancers. Nat Genet. 2000; 24:300–303. [PubMed: 10700188]
2. Rouaux C, Loeffler JP, Boutillier AL. Targeting CREB-binding protein (CBP) loss of function as a therapeutic strategy in neurological disorders. Biochem Pharmacol. 2004; 68:1157–1164. [PubMed: 15313413]
3. Olson EN, Backs J, McKinsey TA. Control of cardiac hypertrophy and heart failure by histone acetylation/deacetylation. Novartis Found Symp. 2006; 274:3–12. discussion 13-19, 152-155, 272-156. [PubMed: 17019803]
4. Jin Q, Yu LR, Wang L, Zhang Z, Kasper LH, Lee JE, Wang C, Brindle PK, Dent SY, Ge K. Distinct roles of GCN5/PCAF-mediated H3K9ac and CBP/p300-mediated H3K18/27ac in nuclear receptor transactivation. Embo J. 2011; 30:249–262. [PubMed: 21131905]
5. Kuo YM, Andrews AJ. Quantitating the specificity and selectivity of Gcn5-mediated acetylation of histone H3. PLoS One. 2013; 8:e54896. [PubMed: 23437046]
6. Henry RA, Kuo YM, Andrews AJ. Differences in specificity and selectivity between CBP and p300 acetylation of histone H3 and H3/H4. Biochemistry. 2013; 52:5746–5759. [PubMed: 23862699]
7. Kalkhoven E. CBP and p300: HATs for different occasions. Biochem Pharmacol. 2004; 68:1145–1155. [PubMed: 15313412]
8. Vo N, Goodman RH. CREB-binding protein and p300 in transcriptional regulation. J Biol Chem. 2001; 276:13505–13508. [PubMed: 11279224]
9. Vander Heiden MG, Cantley LC, Thompson CB. Understanding the Warburg effect: the metabolic requirements of cell proliferation. Science. 2009; 324:1029–1033. [PubMed: 19460998]
10. Tsuchiya Y, Pham U, Hu W, Ohnuma S, Gout I. Changes in Acetyl CoA Levels during the Early Embryonic Development of Xenopus laevis. PLoS One. 2014; 9:e97693. [PubMed: 24831956]
11. Schroeder S, Pendl T, Zimmermann A, Eisenberg T, Carmona-Gutierrez D, Ruckenstuhl C, Marino G, Pietrocola F, Harger A, Magnes C, Sinner F, Pieber TR, Dengjel J, Sigrist SJ, Kroemer G, Madeo F. Acetyl-coenzyme A: A metabolic master regulator of autophagy and longevity. Autophagy. 2014; 10:1335–1337. [PubMed: 24904996]
12. Eisenberg T, Schroeder S, Andryushkova A, Pendl T, Kuttner V, Bhukel A, Marino G, Pietrocola F, Harger A, Zimmermann A, Moustafa T, Sprenger A, Jany E, Buttner S, Carmona-Gutierrez D, Ruckenstuhl C, Ring J, Reichelt W, Schimmel K, Leeb T, Moser C, Schatz S, Kamolz LP, Magnes C, Sinner F, Sedej S, Frohlich KU, Juhasz G, Pieber TR, Dengjel J, Sigrist SJ, Kroemer G, Madeo F. Nucleocytosolic depletion of the energy metabolite acetyl-coenzyme a stimulates autophagy and prolongs lifespan. Cell metabolism. 2014; 19:431444.
13. Gut P, Verdin E. The nexus of chromatin regulation and intermediary metabolism. Nature. 2013; 502:489–498. [PubMed: 24153302]
14. Denisov IG, Sligar SG. A novel type of allosteric regulation: functional cooperativity in monomeric proteins. Arch Biochem Biophys. 2012; 519:91–102. [PubMed: 22245335]

15. Porter CM, Miller BG. Cooperativity in monomeric enzymes with single ligand-binding sites. Bioorg Chem. 2012; 43:44–50. [PubMed: 22137502]
16. Ainslie GR Jr. Shill JP, Neet KE. Transients and cooperativity. A slow transition model for relating transients and cooperative kinetics of enzymes. J Biol Chem. 1972; 247:7088–7096. [PubMed: 4343169]
17. Sweeny JR, Fisher JR. An alternative to allosterism and cooperativity in the interpretation of enzyme kinetic data. Biochemistry. 1968; 7:561–565. [PubMed: 5644128]
18. Mantelingu K, Kishore AH, Balasubramanyam K, Kumar GV, Altaf M, Swamy SN, Selvi R, Das C, Narayana C, Rangappa KS, Kundu TK. Activation of p300 histone acetyltransferase by small molecules altering enzyme structure: probed by surface-enhanced Raman spectroscopy. J Phys Chem B. 2007; 111:4527–4534. [PubMed: 17417897]
19. Bowers EM, Yan G, Mukherjee C, Orry A, Wang L, Holbert MA, Crump NT, Hazzalin CA, Liszczak G, Yuan H, Larocca C, Saldanha SA, Abagyan R, Sun Y, Meyers DJ, Marmorstein R, Mahadevan LC, Alani RM, Cole PA. Virtual ligand screening of the p300/CBP histone acetyltransferase: identification of a selective small molecule inhibitor. Chem Biol. 2010; 17:471–482. [PubMed: 20534345]
20. West AC, Johnstone RW. New and emerging HDAC inhibitors for cancer treatment. J Clin Invest. 2014; 124:30–39. [PubMed: 24382387]
21. Petta V, Gkiozos I, Strimpakos A, Syrigos K. Histones and lung cancer: Are the histone deacetylases a promising therapeutic target? Cancer Chemother Pharmacol. 2013; 72:935–952. [PubMed: 24036844]
22. Barber MF, Michishita-Kioi E, Xi Y, Tasselli L, Kioi M, Moqtaderi Z, Tennen RI, Paredes S, Young NL, Chen K, Struhl K, Garcia BA, Gozani O, Li W, Chua KF. SIRT7 links H3K18 deacetylation to maintenance of oncogenic transformation. Nature. 2012; 487:114–118. [PubMed: 22722849]
23. Russell JC, Amy RM, Graham SE, Dolphin PJ, Wood GO, Bar-Tana J. Inhibition of atherosclerosis and myocardial lesions in the JCR:LA-cp rat by beta, beta'-tetramethylhexadecanedioic acid (MEDICA 16). Arteriosclerosis, thrombosis, and vascular biology. 1995; 15:918–923.
24. Wellen KE, Hatzivassiliou G, Sachdeva UM, Bui TV, Cross JR, Thompson CB. ATP-citrate lyase links cellular metabolism to histone acetylation. Science. 2009; 324:1076–1080. [PubMed: 19461003]
25. Lee JV, Carrer A, Shah S, Snyder NW, Wei S, Venneti S, Worth AJ, Yuan ZF, Lim HW, Liu S, Jackson E, Aiello NM, Haas NB, Rebbeck TR, Judkins A, Won KJ, Chodosh LA, Garcia BA, Stanger BZ, Feldman MD, Blair IA, Wellen KE. Akt-dependent metabolic reprogramming regulates tumor cell histone acetylation. Cell metabolism. 2014; 20:306–319. [PubMed: 24998913]
26. Cornish-Bowden A, Cardenas ML. Specificity of non-Michaelis-Menten enzymes: necessary information for analyzing metabolic pathways. J Phys Chem B. 2010; 114:16209–16213. [PubMed: 21028874]
27. Cai L, Sutter BM, Li B, Tu BP. Acetyl-CoA induces cell growth and proliferation by promoting the acetylation of histones at growth genes. Mol Cell. 2011; 42:426–437. [PubMed: 21596309]
28. Cai L, Tu BP. On acetyl-CoA as a gauge of cellular metabolic state. Cold Spring Harb Symp Quant Biol. 2011; 76:195–202. [PubMed: 21900151]
29. Witt O, Deubzer HE, Milde T, Oehme I. HDAC family: What are the cancer relevant targets? Cancer Lett. 2009; 277:8–21. [PubMed: 18824292]
30. Chateauvieux S, Morceau F, Dicato M, Diederich M. Molecular and therapeutic potential and toxicity of valproic acid. J Biomed Biotechnol. 2010; 2010
31. Kim SC, Chen Y, Mirza S, Xu Y, Lee J, Liu P, Zhao Y. A clean, more efficient method for in-solution digestion of protein mixtures without detergent or urea. J Proteome Res. 2006; 5:3446–3452. [PubMed: 17137347]
32. Garcia BA, Mollah S, Ueberheide BM, Busby SA, Muratore TL, Shabanowitz J, Hunt DF. Chemical derivatization of histones for facilitated analysis by mass spectrometry. NatProtoc. 2007; 2:933–938.

33. Smith CM, Gafken PR, Zhang Z, Gottschling DE, Smith JB, Smith DL. Mass spectrometric quantification of acetylation at specific lysines within the amino-terminal tail of histone H4. Anal Biochem. 2003; 316:23–33. [PubMed: 12694723]

34. Kim Y, Tanner KG, Denu JM. A continuous, nonradioactive assay for histone acetyltransferases. Anal Biochem. 2000; 280:308–314. [PubMed: 10790315]

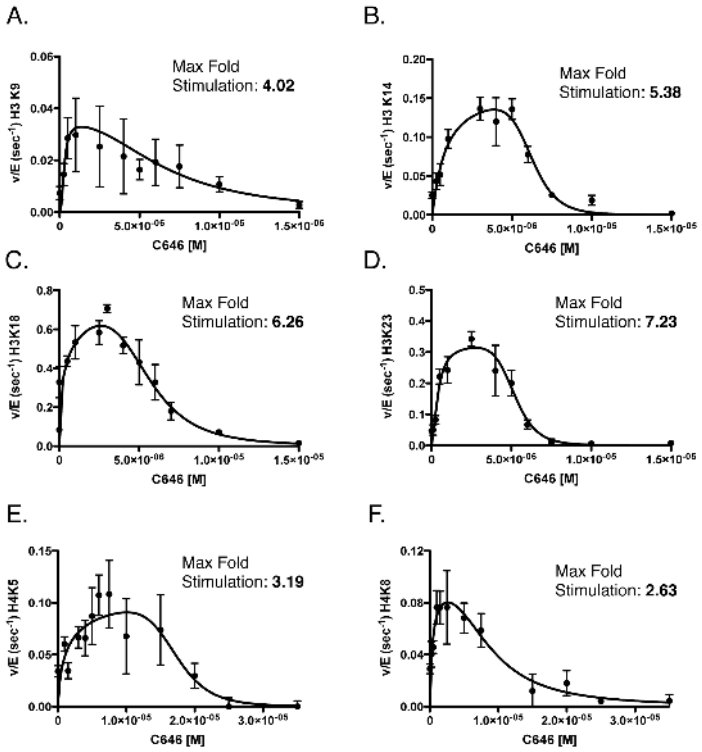

FIGURE 1. C646 mediated changes in p300 acetylation rate under k_{cat} conditions

Experiments were performed in the presence of 200 μM acetyl-CoA, as described in the Methods. The acetylation sites for H3 and H4 are (A-F): H3K9, H3K14, H3K18, H3K23, H4K5, and H4K8. Acetylation of additional sites of H4 can be found in Supplementary Figure 1. The apparent $K_{1/2}$ of activation and inhibition are summarized in Table 1.

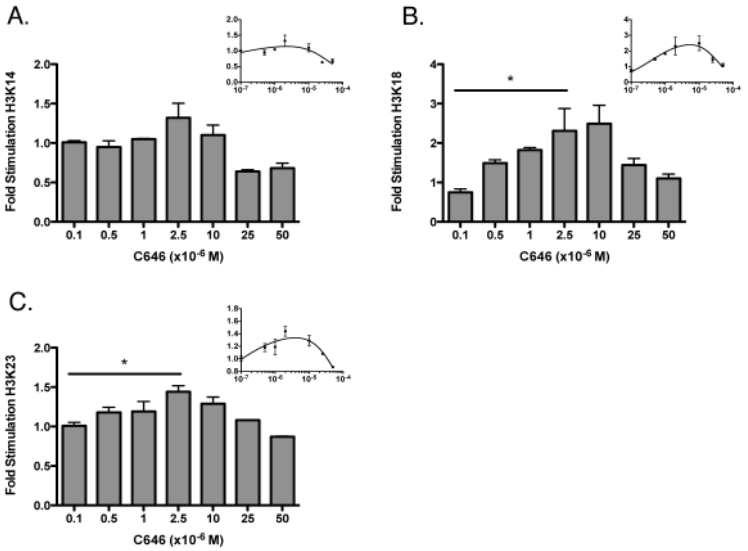

FIGURE 2. Changes in acetylation as a result of C646 treatment in BxPC3 pancreatic cancer cells

BxPC3 cells were treated in triplicate with either a 0.2% DMSO control or varying concentrations of C646 in 0.2% DMSO for 4 hours before harvesting and histone extraction. Acetylation of histone H3 and H4 was analyzed. Each site was normalized to the percentage of acetylation of the DMSO control to show the fold-change in acetylation at that site. The sites shown are (A-C): H3K14, H3K18, and H3K23. The insets show the different C646 concentrations graphed as data points, and a fit line created in the same manner as the *in vitro* data, using Equation 5. A * denotes $p<.05$ from one-way ANOVA for 0.1 to 2.5 μM C646. The results of acetylation for additional sites of H3 and H4 can be found in Supplementary Figure 3, and the apparent EC_{50} and IC_{50}s can be found in Supplementary Table 1.

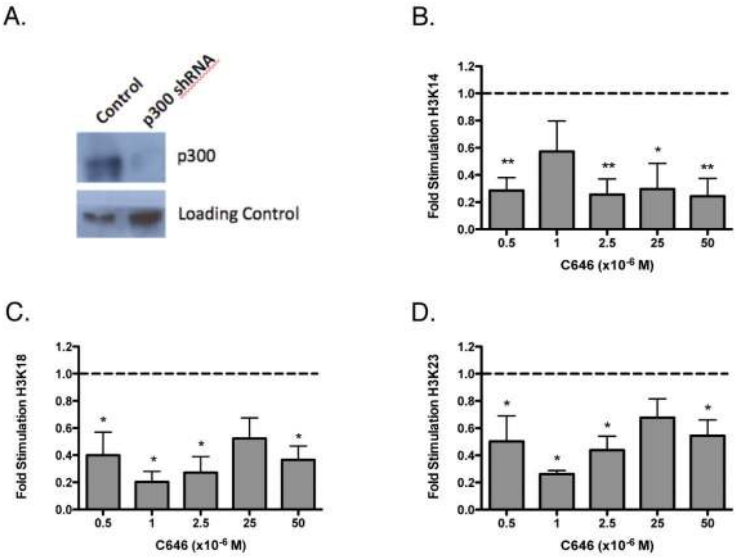

FIGURE 3. Knockdown of p300 in BxPC3 cells causes a loss of the stimulatory effect of C646

BxPC3 cells were treated with shRNA against p300 as described in the Methods. A) Knockdown of p300 was confirmed via Western blot. Alpha-tubulin was used as a loading control. BxPC3 p300 depleted cells were treated in triplicate with either a 0.2% DMSO control or varying concentrations of C646 in 0.2% DMSO for 4 hours before harvesting and histone extraction. Acetylation of histone H3 was analyzed. Each site was normalized to the percentage of acetylation of the DMSO control to show the fold-change in acetylation at that site. The sites shown are (B-D): H3K14, H3K18, and H3K23. * $p < .05$, ** $p < .005$ when compared to the untreated control.

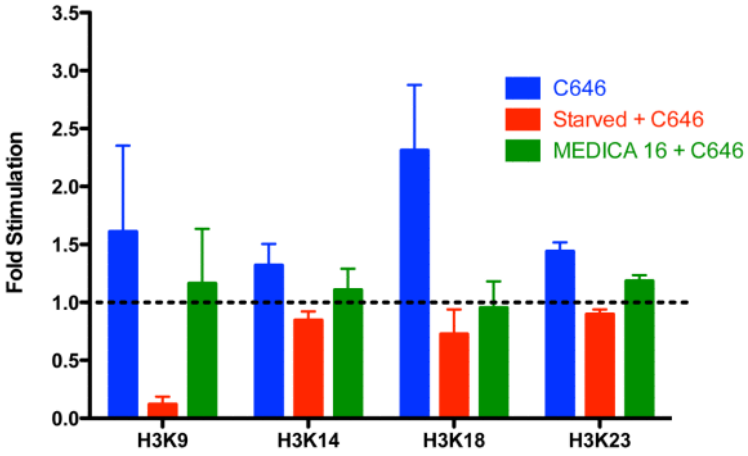

FIGURE 4. C646 inhibition in serum starved cells

BxPC3 cells were treated in triplicate with either a 0.2% DMSO control or 2.5 μM C646 in 0.2% DMSO for 4 hours before harvesting and histone extraction. Acetylation of histone H3 and H4 was analyzed. Each site was normalized to the percentage of acetylation of the DMSO control to show the fold-change in acetylation at that site. Shown are C646 treatments without serum starvation (blue bars), cells that were serum starved 16 hours prior to treatment with C646 (red bars), or cells treated with MEDICA 16 prior to C646 treatment (green bars).

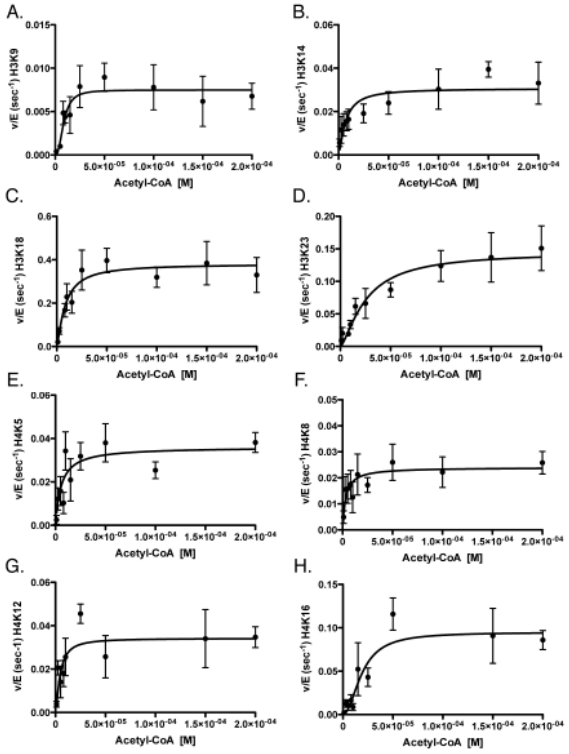

FIGURE 5. Determination of steady-state kinetic parameters of p300-mediated acetylation of histone H3/H4 in the presence of 0.2% DMSO

These experiments, performed with 0.2% DMSO, serve as a control for subsequent C646 steady-state experiments. Shown are the non-linear fits for acetylation at residue A) H3K9, B) H3K14, C) H3K18, D) H3K23, E) H4K5, F) H4K8, G) H4K12, and H) H4K16. The apparent kinetic parameters are summarized in Table 3.

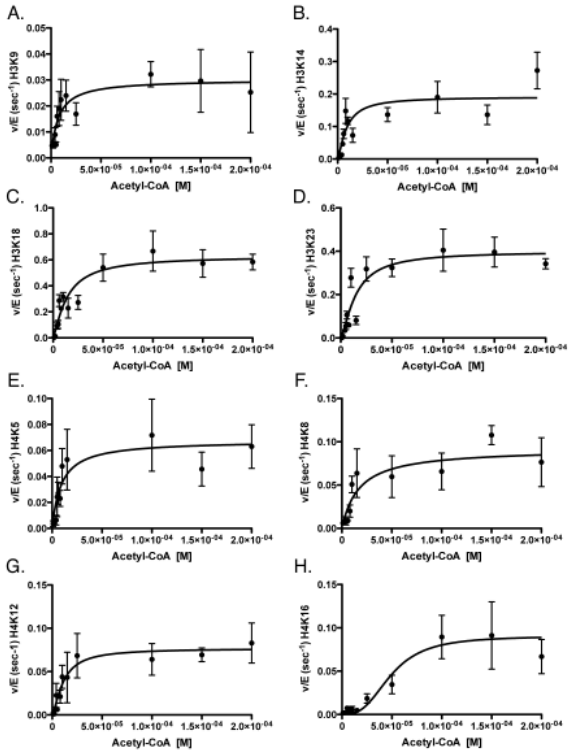

FIGURE 6. Determination of steady-state kinetic parameters of p300-mediated acetylation of histone H3/H4 in the presence of 2.5 μM C646

Shown are the non-linear fits for acetylation at residue A) H3K9, B) H3K14, C) H3K18, D) H3K23, E) H4K5, F) H4K8, G) H4K12, and H) H4K16. The apparent kinetic parameters are summarized in Table 4.

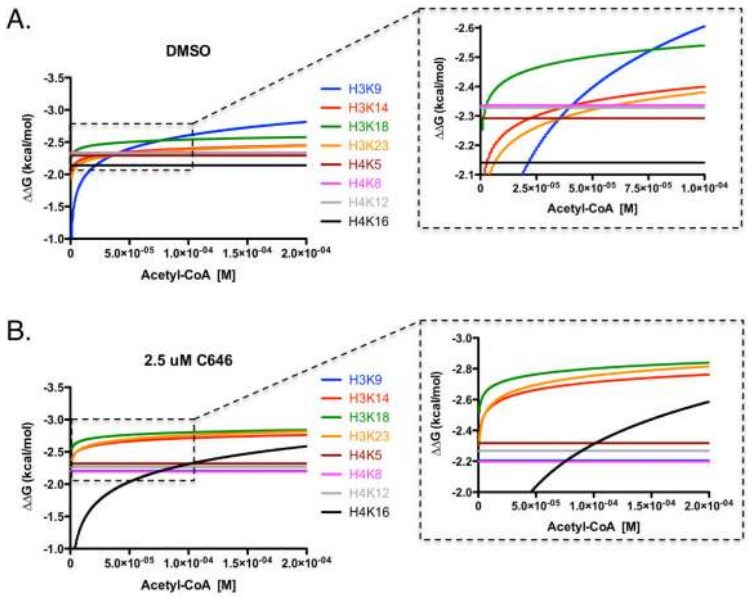

FIGURE 7. ΔΔG of p300 acetylation of H3/H4 sites as a function of acetyl-CoA concentration

The ΔΔG for 8 sites of H3/H4 was calculated from the steady-state parameters determined from Figures 5 and 6. These ΔΔG are graphed as a function of acetyl-CoA concentration in the presence of A) No C646, or B) 2.5 μM C646. Each line indicates how energetically favorable p300 acetylation of a particular residue is, as a function of acetyl-CoA concentration. The intersection points, therefore, indicate the points at which acetylation of one site becomes more favorable than another. The insets show the corresponding graph with the axis zoomed in to better visualize these intersection points. These graphs were also created for 0.5 and 5.0 μM of C646, the results of which can be found in Supplementary Figure 6.

Table 1

$K_{1/2}$ of activation and inhibition for C646 in the presence of p300.

	$K_{1/2\ (activation)}$ ($\times 10^{-6}$ M)	$K_{1/2\ (inhibition)}$ ($\times 10-6$ M)	Maximum Fold Stimulation
H3K9	0.28±0.07	1.37±0.62	4.02
H3K14	0.82±0.34	4.82±0.40	5.38
H3K18	0.27±0.13	2.85±1.39	6.26
H3K23	0.39±0.04	3.25±0.24	7.23
H4K5	1.58±2.75	13.41±3.33	3.19
H4K8	0.38±0.21	3.30±0.99	2.63
H4K12	0.09±0.21	0.88±1.94	1.52
H4K16	0.75±ND	4.70±ND	1.72

* Error could not be determined for H4K16

Table 2

Mean fold-change in acetylation of BxPC3 cells in the presence of drug treatment, with and without 16 hours of serum starvation.

	C646 (2.5 μM)	C646 (Starved)	TSA (0.5 μM)	TSA (Starved)
H3K9	1.61	0.12	68.56	3.02
H3K14	1.32	0.84	2.412	1.65
H3K18	2.31	0.72	14.87	1.94
H3K23	1.44	0.89	2.83	1.78

Table 3

Steady-state parameters of H3 and H4 for p300-mediated acetylation of H3/H4 in the presence of 0.2% DMSO.

	k_{cat} ($\times 10^{-3}$ sec^{-1})	$K_{1/2}$ ($\times 10^{-6}$ M)	$k_{cat}/K_{1/2}$ ($\times 10^{3}$ $M^{-1}sec^{-1}$)	nH (Hill Coefficient)	$k_{cat}/K_{1/2}^{nH}$ ($M^{-nH}sec^{-1}$)
H3K9	7.48±0.42	8.64±1.05	0.87±0.12	2.43±0.72	(1.42±0.19) $\times 10^{10}$
H3K14	30.62±6.38	7.02±4.96	4.36±3.21	1.34±0.17	(2.35±1.24) $\times 10^{5}$
H3K18	380.5±17.28	8.44±1.33	45.09±7.41	1.26±0.1	(8.97±7.40) $\times 10^{5}$
H3K23	145±13.17	25.73±6.16	5.64±1.44	1.41±0.12	(4.16±3.19) $\times 10^{5}$
H4K5	36.07±2.56	5.61±1.52	6.43±1.8	n.a.	n.a.
H4K8	23.99±1.22	3.02±0.75	7.95±2.03	n.a.	n.a.
H4K12	35.88±2.34	4.71±1.22	7.62±2.03	n.a.	n.a.
H4K16	32.35±1.94	10.35±2.24	3.13±0.7	n.a.	n.a.

Table 4

Steady-state parameters of H3 and H4 for p300-mediated acetylation of H3/H4 in the presence of 2.5 μM C646.

	k_{cat} ($\times 10^{-3}$ sec^{-1})	$K_{1/2}$ ($\times 10^{-6}$ M)	$k_{cat}/K_{1/2}$ ($\times 10^{3}$ $M^{-1}sec^{-1}$)	nH (Hill Coefficient)	$k_{cat}/K_{1/2}^{nH}$ ($M^{-nH}sec^{-1}$)
H3K9	30.17±1.87	7.11±1.61	4.24±1	n.a.	n.a.
H3K14	191.3±7.43	9.02±1.04	21.2±2.59	1.34±0.17	(1.05±0.52) $\times 10^{6}$
H3K18	629.2±22.73	14.22±1.51	44.25±4.95	1.26±0.1	(7.70±6.64) $\times 10^{5}$
H3K23	399±12.08	14.81±1.37	26.94±2.62	1.41±0.12	(2.49±1.81) $\times 10^{6}$
H4K5	67.68±5.33	9.29±2.11	7.28±1.75	n.a.	n.a.
H4K8	98.27±7.02	23.97±5.55	4.1±0.99	n.a.	n.a.
H4K12	83.73±5.98	14.63±3.05	5.72±1.26	n.a.	n.a.
H4K16	90.43±7.03	49.11±6.59	1.84±0.29	2.89±0.85	(2.56±0.36) $\times 10^{11}$